Journal of Fluorine Chemistry 132 (2011) 63–67

Contents lists available at ScienceDirect

Journal of Fluorine Chemistry

journal homepage: www.elsevier.com/locate/fluor

Thermal rearrangement of substituted difluoro(methylene)cyclopropane

Xiao-Chun Hang [a], Wei-Peng Gu [a], Qing-Yun Chen [a], Ji-Chang Xiao [a,*], Wei-Guo Xu [b], Shubin Liu [c]

[a] Key Laboratory of Organofluorine Chemistry, Shanghai Institute of Organic Chemistry, Chinese Academy of Sciences, 345 Lingling Road 200032, China
[b] Zhejiang Chemical Industry Research Institute, 387 Tianmushan Road, Hangzhou, Zhejiang 310023, China
[c] Research Computing Center, University of North Carolina, Chapel Hill, NC 27599-3420, USA

ARTICLE INFO

Article history:
Received 23 July 2010
Received in revised form 15 November 2010
Accepted 16 November 2010
Available online 24 November 2010

Keywords:
Difluoro(methylene)cyclopropane
Thermal rearrangement
DFT calculations
Transition state

ABSTRACT

Both experimental and computational approaches have been employed in the present work to investigate the thermal conversion of substituted difluoro(methylene)cyclopropanes (F_2MCP) E-1,1-difluoro-2,2-dimethyl-3-tosylmethylene cyclopropane **1**, to the thermodynamically more stable F_2MCP products, 1,1-difluoro-2-tosyl-3-(propan-2-ylidene)cyclopropane **2**, and 1-(3-(difluoromethylene)-2,2-dimethylcyclopropylsulfonyl)-4-methylbenzene **3**. The X-ray crystal structure has been obtained for both **1** and **2**, respectively, based on which theoretical analyses on their structure and stability have been carried out. Possible reaction mechanisms are proposed.

1. Introduction

Thermal rearrangement of methylenecyclopropane (MCP) derivatives has been of continuous recent interest in the literature and trimethylenemethane (TMM) intermediates are often considered to be produced in the rearrangement process [1]. There are two different kinds of TMM conformations in the form of conjugated diradicals, and dipolar processes can be undertaken under the thermal conditions, which have been well studied in the past decades [2]. It is well known that introduction of fluorine atoms into organic molecules causes special electrostatic and steric consequences [3]. For this reason, the investigation of fluorinated MCPs rearrangements has generated considerable interests in the literature [4]. Recently, we discovered that the difluoro(methylene)cyclopropanes (F_2MCPs) can be readily prepared from the direct difluorocyclopropanation of sulfonylated allenes [5]. This class of F_2MCPs has a particularly interesting skeleton substituted by both electron-donating methyl and electron-withdrawing tosyl groups. During the difluorocarbene addition process, carbene has been revealed to exclusively add to the electron-rich double bond via the kinetically controlled process as recently vindicated by computational studies in the literature [4], giving the F_2MCP (E)-1,1-difluoro-2,2-dimethyl-3-tosylmethylenecyclopropane **1** as the product [6]. In this work, we examine the thermal stability of this F_2MCP by both experimental and computational approaches.

2. Results and discussion

Thermolysis of **1** at 120 °C in chloroform for three days resulted in the diminution of the singlet fluorine signal intensity in ^{19}F NMR spectra at −138.4 ppm and the appearance of several new peaks. Product isolation, purification and characterization demonstrated that **1** was rearranged to **2** and **3** with the yield of 45% and 30%, respectively (Scheme 1). The same rearrangement reaction can also take place in other solvents such as methanol and toluene, giving almost the same ratio of **2**–**3**. It should be noted that F_2MCP **1** was synthesized by the addition of difluorocarbene to 1-tosyl-3,3-dimethyl allene at 120 °C and the reaction was completed within 2 h, where the formation of **2** was not observed (Scheme 2). With putting the above together, this rearrangement reaction provides a good manifestation of the chemical characteristics of difluorocarbene whose addition reaction has been shown earlier to favor the electron rich alkenes [7]. That is, the addition of difluorocarbene to 1-tosyl-3,3-dimethyl allene leading to **1** should be is a kinetically controlled process.

X-ray crystallographic analysis of **1** and **2** was carried out (Figs. 1 and 2) [8]. Thermal rearrangement of **1** into **2** involves the cleavage of C3–C4 bond, which has a normal bond length (1.4863 Å), while several carbon–carbon bonds in the three-membered ring structure such as C2–C4 of F_2MCP **1** and C1–C2 of F_2MCP **2** are found to be longer than the distal bond of F_2MCPs **1** (numbering of carbon atoms: see Figs. 1 and 2). The fact that the C3–C4 bond in **1** breaks in the thermal conversion process of **1** into

* Corresponding author at: Shanghai Institute of Organic Chemistry, CAS Key Laboratory of Organofluorine Chemistry, 354, Fenglin Road, Shanghai, China. Tel.: +86 21 54925340; fax: +86 21 64166128.
E-mail addresses: jchxiao@mail.sioc.ac.cn (J.-C. Xiao), shubin@email.unc.edu (S. Liu).

0022-1139/$ – see front matter © 2010 Elsevier B.V. All rights reserved.
doi:10.1016/j.jfluchem.2010.11.007

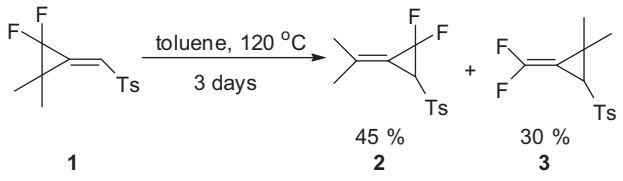

Scheme 1. Thermal rearrangement of F_2MCP **1**.

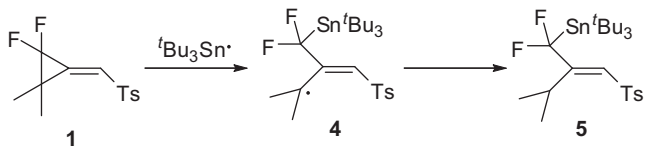

Scheme 3. The reaction of **1** with radical.

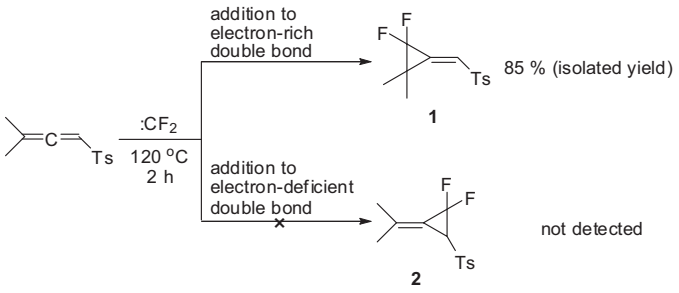

Scheme 2. Addition of difluorocarbene to 1-tosyl-3,3-dimethyl allene.

2 suggests the possibility of energetically favorable C3–C4 bond cleavage process.

Two mechanisms for the above conversion would be possible, one via radical intermediate and the other through polar intermediate, although there is no direct experimental evidence to determine this process. Our earlier results suggested that the distal bond can be opened under the stannyl radical condition, giving rise to the ring-opened addition product **5** via the radical pathway (Scheme 3) [9].

To better understand the relative stability of **1** and **2** and their conversion, theoretical approach was carried out. Density functional theory (DFT) calculations at the B3LYP/6-311+G(d) level of theory were performed using Gaussian 03E01 package [10] to study the structure of **1**, **2**, and **3**, and the transition state TS1 (from **1** to **2**) and TS2 (from **1** to **3**). The optimized structures of TS1 and TS2 are shown in Fig. 3.

Shown in Table 1 are a few selected structural parameters from the optimized structures together with X-ray data. The main difference between **1** and **2** is that the 3-membered cyclopropane ring and the two methyl groups (i.e., 5 carbon atoms in total) are in the same plane in **2**, whereas in **1**, they are in the almost perpendicular position. This difference can be seen from the CF2–C2–C4–CH3 (see Fig. 1 for the numbering sequence of the carbon atoms) dihedral angle in Table 1, where in **2** the value is close to 0° (8.7 from theory and 14.0 from the X-ray structure) and in **1** it is about 107°. The value of the dihedral angle in the transition state (TS1) falls just in-between, giving 65.3° (Fig. 3). The structural difference between **1** and **3** is small where the dihedral angle between the ring and two methyl groups in **3** is also far from 0° (64.4°). Computational results agree well with experimental data.

These structural differences dedicate the stability difference of these compounds. The nature of the stability difference can be discussed by hyperconjugation effects [11]. It was quantitatively examined by the second-order perturbation theory analysis of the Fock matrix in the NBO basis (Table 2). It is likely that the conversion reaction site from **1** to **2** consists of three relatively independent components from the viewpoint of the classical Lewis structure: a C=C double bond, a cyclopropane ring and methyl groups. The

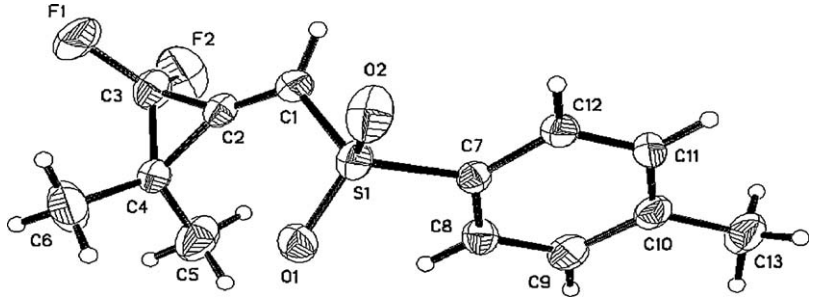

Fig. 1. The single crystal structure of F_2MCPs **1**. Selected bond lengths [Å], bond angles [°]: C(1)–C(2) 1.307(3), C(2)–C(3) 1.447(3), C(2)–C(4) 1.488(2), C(3)–C(4) 1.486(3); C(1)–C(2)–C(3) 148.7(2), C(1)–C(2)–C(4) 150.4(2), C(3)–C(2)–C(4) 61.84(17), C(2)–C(3)–C(4) 60.93(16); C(3)–C(4)–C(2) 58.23(15).

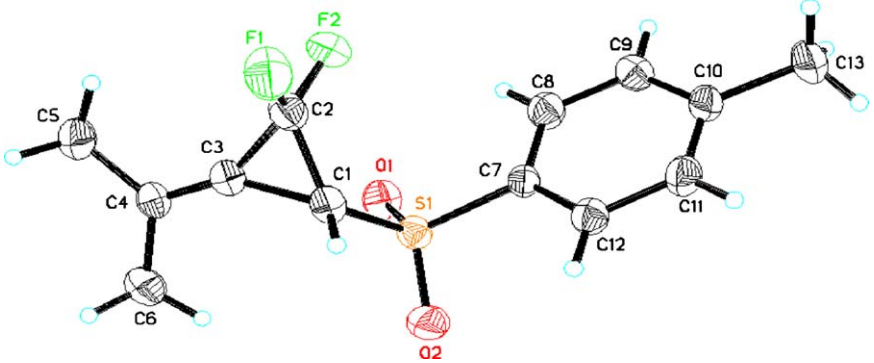

Fig. 2. Single crystal structures of F_2MCPs **2**. Selected bond lengths [Å], bond angles [°]: C(1)–C(2) 1.500(3), C(1)–C(3) 1.487(3), C(2)–C(3) 1.416(3), C(3)–C(4) 1.314(3); C(1)–C(2)–C(3) 61.22(14), C(4)–C(3)–C(2) 150.6(2), C(4)–C(3)–C(1) 145.7(2), C(2)–C(3)–C(1) 62.17(14); C(3)–C(1)–C(2) 56.60(14).

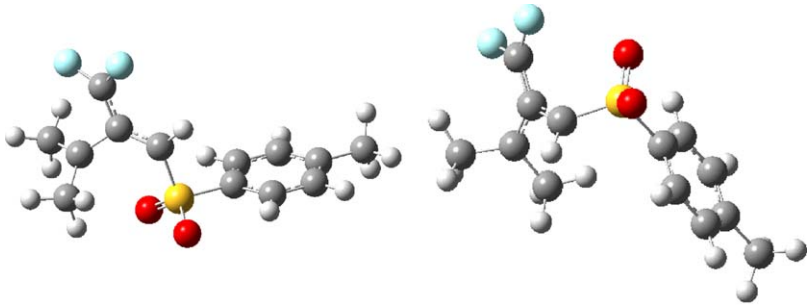

Fig. 3. The optimized structure of the thermal conversion transition states, TS1 (**1** → **2**) and TS2 (**1** → **3**).

Table 1
Comparison of selected optimized structure parameters of **1** and **2** as well as their conversion transition state. Data in parenthesis are from X-ray crystal structures. See the main text for detailed discussions.

Structure parameters	1	2	3	TS1	TS2
C2–C3	1.4613	1.4384			
Bond length (Å)	(1.4476)	(1.4161)	1.3072	1.3881	1.3886
C3–C4/C1–C2	1.5099	1.5155			
Bond length (Å)	(1.4868)	(1.5005)	–	–	–
CF_2–C2–C4–CH_3	107.7	8.7			
Dihedral angle (°)	(107.6)	(14.0)	64.4	65.3	84.4

Table 2
Comparison of second-order perturbation theory analysis and energy decomposition analysis for **1** and **2** as well as their conversion transition state. See the main text for detailed discussions. Energy differences units in kcal/mol.

	1	2	3	TS1	TS2
Second-order perturbation theory analysis (kcal/mol)					
C=C and cyclopropane ring	43.30	47.21	41.37		
Cyclopropane and methyl groups	9.32	20.15	17.42		
C=C and methyl groups	10.48	10.25	10.90		
Hyperconjugations (sum of above)	63.10	77.61	69.69		
Energy decomposition analysis					
Steric energy difference	0.00	−7.04	−85.53	−17.83	54.15
Quantum energy difference	0.00	11.09	82.24	20.98	−45.46
Electrostatic energy difference	0.00	−7.32	1.68	30.40	28.09
Kinetic energy difference	0.00	5.21	0.22	−32.90	−36.73
Exc energy difference	0.00	−1.15	−3.50	36.05	45.43
Total energy difference	0.00	−3.26	−1.60	33.55	36.77

conversion from **1** to **3** can be analyzed similarly. The second-order perturbation theory in NBO analysis is able to find out the interaction energy between each pair of these three molecular motifs.

From Table 2, it is obvious that there are much stronger hyperconjugation interactions in **2** (77.61 kcal/mol in total) than in **1** (63.10 kcal/mol in total), 14.51 kcal/mol in difference, which would contribute to the stability of **2** as compared with **1**. Compound **3** (69.69 kcal/mol in total) also has a larger hyperconjugation effect than **1**, but smaller than **2**. Taking a closer look of these data in Table 2, we found that the major factor for energy difference between **1** and **2** and between **1** and **3** is the hyperconjugation interaction between the σ bonding orbital of the electron-donating two methyl groups and the σ^* antibonding orbital of the electron-deficient cyclopropane ring. Calculated data showed a slightly more favorable interaction in **2** as compared with **3**, which possibly explain the difference in the yield (product ratio) in the thermal conversion of **1** (45% of **2** vs. 30% of **3**). It is noted that the distance between the cyclopropane (C1–C2–C3) ring and the methyl groups (C5 and C6) in **2** is indeed longer than that in **1**. The stronger hyperconjugation interactions between these two groups in **2** would be a result from the fact that all five aforementioned carbon atoms in **2** are in the same plane, facilitating bonding molecular orbitals to overlap with antibonding MOs, which is the main feature of the hyperconjugation interaction among MOs.

Also shown in Table 2 is the energy decomposition analysis [12], where contributions from steric, quantum, and electrostatic effects can be unambiguously quantified. This kind of analysis is able to tell us what kind of the effects comes into play as the factor or factors governing the overall energy difference. It was observed that for the conversion from **1** to **2**, less steric hindrance is resulted, though the transition state has even smaller steric repulsion. This result is consistent with the NBO steric energy [13–15] from a different quantification scheme of the steric effect (see Table 2, steric energy difference). Compound **2** was also found to have lower electrostatic interaction, but larger quantum effect. The total energy difference between **1** and **2** at the DFT B3LYP/6-311+G(d) level of theory is −3.26 kcal/mol, indicating that **2** is more stable than **1** and thermal rearrangement of Scheme 1 is a thermodynamically favorable process. In addition, the barrier height of the transition state is 33.55 kcal/mol, which is consistent with the computational results from the literature [5]. For the pathway from **1** to **3**, the barrier height is larger, 36.77 kcal/mol. Compound **3** has much smaller steric repulsion than both **1** and **2**, but it is compensated by the larger repulsive quantum contribution due to exchange-correlation effects. It should be worthy to note that heating of the isolated **2** at 120 °C for 3

days in chloroform, toluene, DMSO or an ionic liquid [BMIM][PF_6] resulted in a complete recovery of **2**.

3. Conclusion

The present work presents the thermal rearrangement of F_2MCP **1** to thermodynamically more stable products **2** and **3**. In addition to the X-ray crystal structures of these compounds, theoretical analyses on their structure and stability have been performed. Our computational study at the DFT B3LYP/6-311+G(d) level of theory clearly supported the present experimental results.

4. Experimental

4.1. General information

^{1}H NMR spectra were recorded on a Bruker AM 300 (300 MHz) spectrometer with TMS as an internal standard (negative for upfield). ^{19}F NMR spectra were recorded on a Bruker AM 300 (282 MHz) with $CFCl_3$ as an external standard (negative for upfield). ^{13}C NMR spectra were recorded on a Bruker AM 300 (75 MHz) spectrometer with $CDCl_3$ as an internal standard (negative for upfield). MS and HRMS were recorded on a Hewlett–Packard HP-5989A spectrometer and a Finnigan MAT-8483 mass spectrometer. Elemental analyses were obtained on a Perkin–Elmer 2400 Series II Elemental Analyzer. Infrared spectra were measured with a Perkin–Elmer 983 spectrometer. TLC analyses were performed on silica gel plates (RP-18 WF_{254s}, Merck, 0.25 mm), and column chromatography was performed using silica gel (mesh 300–400). All solvents were purified by standard methods. $FSO_2CF_2COOSiMe_3$ (TFDA) [1], sulfonyl allenes [2], [bmim]PF_6 [3] were prepared as described in the literature.

4.2. General procedure for the synthesis of compound 1

1-Methyl-4-(3-methylbuta-1,2-dienylsulfonyl)benzene (2 g, 9.2 mmol), NaF (38 mg, 10 mol%) and xylene (20 mL) were placed under N_2 in a three-necked flask fitted with a magnetic stirring bar and a pressure-equalizing dropping funnel. After the mixture was heated to 120 °C (oil bath), TFDA (5.75 g 2.5 equiv.) diluted in 5 mL xylene was added dropwise within a period of about 1 h. The mixture was then stirred for an additional 1 h to ensure the consumption of the substrate. After being cooled to room temperature, the solvent was removed under reduced pressure. The residue was purified by chromatography on a silica gel column (petroleum ether:ethyl acetate = 10:1) to yield **1** as a solid (2.1 g, 85%). ^{1}H NMR (300 MHz, $CDCl_3$): δ = 1.45 (t, J = 1.5 Hz, 6H), 2.46 (s, 3H), 7.00 (s, 1H), 7.37 (d, J = 8.1 Hz, 2H), 7.80 (d, J = 8.1 Hz, 2H) ppm. ^{19}F NMR (282 MHz, $CDCl_3$): δ = –138.7 (s, 2F) ppm. ^{13}C NMR (100 MHz, $CDCl_3$): δ 17.5, 21.9, 31.8 (t, J_{FC} = 10.8 Hz), 107.6 (t, J_{FC} = 297.0 Hz), 126.4, 128.2, 130.4, 137.0, 144.0 (t, J_{FC} = 8.2 Hz), 145.6. IR (film): 2982, 1744, 1594, 1490, 1461, 1394, 1342, 1322, 1298, 1239, 1210, 1154 cm^{-1}. MS (EI): m/z: 272 (100) [M^+]. Anal. calcd. for $C_{13}H_{14}F_2O_2S$: C 57.34, H 5.18; found: C 57.37, H 5.17.

4.3. General procedure for thermal isomerization of compound 1

A 5 mL sealed tube was charged with **1** (54 mg, 0.20 mmol) and chloroform (1.0 mL). The sample was stirred at 120 °C for 3 d. After being cooled to room temperature, the solvent was removed under reduced pressure. The residue was firstly purified by chromatography on a silica gel column (petroleum ether:ethyl acetate = 10:1) to give the products **2** and **3** as a mixture. Then the mixture was separated by HPLC to obtain **2** (24 mg, 45%) and **3** (16 mg, 30%), respectively. F_2MCP **2**: mp. 82–84 °C. ^{1}H NMR (300 MHz, $CDCl_3$): δ 2.06–2.14 (m, 6H), 2.47 (s, 3H), 3.65–3.76 (m, 1H), 7.38 (d, J = 7.8 Hz, 2H), 7.83 (d, J = 7.8 Hz, 2H). ^{19}F NMR (282 MHz, $CDCl_3$): δ −120.96 (d, J = 152.4 Hz, 1F), −135.84 (d, J = 152.4 Hz, 1F). ^{13}C NMR (100 MHz, $CDCl_3$): δ 21.7, 23.1, 23.7, 48.5 (t, J_{FC} = 17.8 Hz), 99.4–106.7 (m, 2C), 128.0, 130.0, 137.2, 145.1, 145.8. IR (film): 3545, 3485, 3086, 2926, 2856, 1598, 1444, 1312, 1192, 1161, 1141, 1086, 1052, 1014, 989, 715, 656, 585, 571, 518 cm^{-1}. MS (ESI): m/z 290.3 [M+Na$^+$]. F_2MCP **3**: ^{1}H NMR (300 MHz, $CDCl_3$): δ 1.31 (s, 3H), 1.67 (s, 3H), 2.46 (s, 3H), 3.04 (s, 1H), 7.37 (d, J = 8.2 Hz, 2H), 7.81 (d, J = 8.2 Hz, 2H). ^{19}F NMR (282 MHz, $CDCl_3$): δ −81.50 (dd, J_1 = 51.6 Hz, J_2 = 4.3 Hz, 1F), −79.82 (d, J = 51.6 Hz, 1F). ^{13}C NMR (100 MHz, $CDCl_3$): δ 17.8, 21.6, 25.6, 29.1, 48.2 (t, J_{FC} = 6.7 Hz), 127.7, 129.9, 138.3, 144.8, 151.2. IR (film): 2964, 2928, 1843, 1598, 1462, 1261, 1147, 1087, 1018, 801, 660, 576 cm^{-1}. MS (ESI): m/z 326.9 [M+MeOH+Na$^+$], HRMS (ESI) calcd. for $C_{13}H_{14}O_2F_2S^+$: 272.0683; found: 272.0690.

4.4. Computational details

High-level density functional theory (DFT) calculations using the B3LY approximate exchange-correlation energy density functional have been performed with the standard Pople basis set 6-311 + G* for all elements. Calculations were performed in both the gas phase at 0 K temperature and in the chloroform solvent using the implicit solvent model, IEF-PCM (the integral equation formalism of the polarizable continuum model) with tight SCF convergence and ultrafine integration grids. For stable structure optimizations, a single-point frequency calculation was carried out after each optimization to make sure that there is no negative frequency. For transition-state structure searches, the single-point frequency calculation subsequently performed is to ensure that the final transition state structure obtained has only one imaginary frequency and the vibration mode of the negative frequency corresponds to the bond formation that is anticipated. In addition, intrinsic reaction coordinates (IRC) were calculated to verify the relevance of transition-state structures. The natural bond orbital and charge analysis was performed using the second-order perturbation theory analysis of the Fock matrix in the NBO basis to examine the hyperconjugation interactions between different chemical bonds. The energy decomposition analysis was also employed in this work [12,15].

Acknowledgements

We thank the Chinese Academy of Sciences (Hundreds of Talents Program) and the National Natural Science Foundation (20972179 and 21032006) for financial support. The authors also acknowledge the use of the computational resources provided by Research Computing Center at University of North Carolina at Chapel Hill for the present study.

References

[1] (a) E.F. Ullman, J. Am. Chem. Soc. 82 (1960) 505–506;
(b) J.C. Gilbert, J.R. Butler, J. Am. Chem. Soc. 92 (1970) 2168–2169;
(c) J.J. Gajewski, J. Am. Chem. Soc. 90 (1968) 7178–7179;
(d) J.J. Gajewski, J. Am. Chem. Soc. 93 (1971) 4450–4458.
[2] (a) L. Birladeanu, Tetrahedron 29 (1973) 499–512;
(b) J.J. Gajewski, S.K. Chou, J. Am. Chem. Soc. 99 (1977) 5696–5707;
(c) J.J. Gajewski, C.W. Benner, B.N. Stahly, R.F. Hall, R.I. Sato, Tetrahedron 38 (1982) 853–862.
[3] (a) P. Kirsch, Modern Fluoroorganic Chemistry, Wiley-VCH, Weinheim, Germany, 2004;
(b) R.D. Chambers, Fluorine in Organic Chemistry, Blackwell, Cambridge, MA, 2004.
[4] (a) W.R. Dolbier, T.H. Fielder, J. Am. Chem. Soc. 100 (1978) 5577–5578;
(b) W.R. Dolbier, C.R. Burkholder, J. Am. Chem. Soc. 106 (1984) 2139–2142;
(c) W.R. Dolbier, C.R. Burkholder, A.L. Chaves, A. Green, J. Fluorine Chem. 77 (1996) 31–37;
(d) W.R. Dolbier, E. Gautriaud, X. Cai, J. Fluorine Chem. 126 (2005) 339–343;
(e) W.R. Dolbier, Acc. Chem. Res. 14 (1981) 195–200;

(e) S.B. Lewis, D.A. Hrovat, S.J. Getty, W.T. Borden, J. Chem. Soc. Perkin Trans. 2 (1999) 2339–2347;
(g) H. Wei, D.A. Hrovat, W.T. Borden, J. Am. Chem. Soc. 128 (2006) 2497–16676.
[5] Z.-L. Cheng, J.-C. Xiao, C. Liu, Q.-Y. Chen, Eur. J. Org. Chem. (2006) 5581–5587.
[6] (a) X.-C. Hang, Q.-Y. Chen, J.-C. Xiao, Eur. J. Org. Chem. (2008) 1101–1106;
(b) X.-C. Hang, Q.-Y. Chen, J.-C. Xiao, Synlett (2008) 1989–1992.
[7] (a) B.E. Smart, in: M. Hudlicky, A.E. Pavlath (Eds.), In Chemistry of Organic Fluorine Compounds II, American Chemical Society, Washington, DC, 1995;
(b) D.L.S. Brahms, W.P. Dailey, Chem. Rev. 96 (1996) 1585–1632;
(c) F. Tian, V. Kruger, O. Bautista, J.-X. Duan, A.-R Li, W.R. Dolbier Jr., Q.-Y Chen, Org. Lett. 2 (2000) 563–564.
[8] CCDC 720067 and CCDC 659840 contain the supplementary crystallographic data for the compound 1 and 2. This data can be obtained free of charge via www.ccdc.cam.ac.uk/data_request/cif.
[9] (a) X.-C. Hang, Q.-Y. Chen, J.-C. Xiao, J. Org. Chem. 73 (2008) 8598–8600;
(b) X.-C. Hang, W.-P. Gu, Q.-Y. Chen, J.-C. Xiao, Tetrahedron 65 (2009) 6320–6324.
[10] M.J. Frisch, G.W. Trucks, H.B. Schlegel, G.E. Scuseria, M.A. Robb, J.R. Cheeseman, J.A. Montgomery Jr., T. Vreven, K.N. Kudin, J.C. Burant, Gaussian 03, Revision E. 01, Gaussian, Inc, Pittsburgh, PA, 2003.
[11] P.R. Schreiner, Angew. Chem. Int. Ed. 41 (2002) 3579–3581.
[12] (a) S.B. Liu, J. Chem. Phys. 126 (2007) 19110–19112;
(b) S.B. Liu, N. Govind, J. Phys. Chem. A 112 (2008) 6690–6699.
[13] J.K. Badenhoop, F. Weinhold, J. Chem. Phys. 107 (1997) 5406–5421.
[14] P.K. Chattaraj, U. Sarkar, D.R. Roy, Chem. Rev. 106 (2006) 2065–2091.
[15] (a) S.B. Liu, J. Chem. Sci. 117 (2005) 477–483;
(b) G. Zhong, C.Y. Rong, S.B. Liu, J. Phys. Chem. A 111 (2007) 3132–3136;
(c) Y. Xia, D.L. Yin, C. Rong, D. Xu, D. Yin, S.B. Liu, J. Phys. Chem. A. 112 (2008) 9970–9977;
(d) S.B. Liu, W. Langenaeker, Theor. Chem. Acc. 110 (2003) 338–344;
(e) Y. Huang, A.G. Zhong, C. Rong, X.M. Xiao, S.B. Liu, J. Phys. Chem. A 112 (2008) 305–311.